

Born-form approximation and full one-loop results for $e^+e^- \rightarrow W^+W^- \rightarrow 4$ fermions $(+\gamma)^{*†}$

Masaaki Kuroda

Department of Physics, Meiji-Gakuin University,
Yokohama 244, Japan

and

Dieter Schildknecht

Department of Physics, University of Bielefeld,
Universitätsstraße 25, D-33615 Bielefeld, Germany

Abstract

We review the results on representing the differential cross section for W-pair production, including W decay and hard-photon bremsstrahlung, in terms of a Born-form approximation of fairly simple analytic form. The results of the Born-form approximation are compared with full-one-loop results. The emphasis is on the energy range of future e^+e^- (or $\mu^+\mu^-$) colliders.

BI-TP 2000/05

*Presented by D. Schildknecht at the ECFA/DESY Linear Collider Workshop, Oberrnai, 16-19th October, 1999, to appear in the Workshop Proceedings.

†Supported by the Bundesministerium für Bildung und Forschung, No.05HT9PBA2, Bonn, Germany

1 Introduction

I will start with a few remarks on W-pair production at LEP energies based on work [1] in collaboration with Masaaki Kuroda and Ingolf Kuss. Subsequently, I will turn to W-pair production at the energy range of future e^+e^- (or $\mu^+\mu^-$) colliders. Specifically, the talk will be based on recent work in collaboration with Masaaki Kuroda and Y. Kurihara [2, 3, 4]. The high-energy-Born-form approximation (HEBFA) is compared with full-one-loop results including W-decay. The double-pole approximation employed throughout is explicitly justified by demonstrating its validity, provided appropriate cuts are introduced on the two-fermion invariant masses. As a consequence of the strong increase with energy of the virtual corrections involving the non-Abelian couplings, even limited experimental accuracy at TeV energies will be seen to be sufficient to isolate their effects. For elaborate work on W-pair production, on various aspects more complete than the work presented here, I would like to refer to the talks by A. Denner [5] and A. Vicini at this meeting.

2 The Born Approximation

The Born approximation for the reaction $e^+e^- \rightarrow W^+W^-$, based on the well-known s-channel, (γ, Z_0) -exchange and t-channel, ν -exchange diagrams may be written as (e.g. [1])

$$\mathcal{M}_{Born}(\sigma, \lambda_+, \lambda_-, s, t) = g_{W^\pm}^2 \frac{1}{2} \delta_{\kappa^-} \mathcal{M}_I + e^2 \mathcal{M}_Q, \quad (1)$$

where the dependence on energy and momentum transfer squared, s and t , and on twice the electron and the W^\pm helicities, $\sigma = \pm 1$ and $\lambda_\pm = 0, \pm 1$, is contained in the basic matrix elements \mathcal{M}_I and \mathcal{M}_Q . The calculation of the cross section for $e^+e^- \rightarrow W^+W^-$ in (1) requires the specification of an appropriate energy scale at which the SU(2) coupling, g_{W^\pm} and the electromagnetic coupling, e are to be defined. For W-pair production at LEP2 energies of $2M_{W^\pm} \lesssim \sqrt{s} \lesssim 200 GeV$, it is natural to choose a high-energy scale, such as \sqrt{s} , or, with sufficient accuracy, $M_W \simeq M_Z$ instead of \sqrt{s} . Accordingly, we have

$$\left(\frac{e^2}{4\pi}\right)^{-1} = \alpha^{-1}(M_Z^2) = 128.89 \pm 0.09 \quad (2)$$

for the electromagnetic coupling, while $g_{W^\pm}^2(M_{W^\pm}^2)$ is obtained [1] from the leptonic width of the W^\pm

$$g_{W^\pm}^2(M_{W^\pm}^2) = 48\pi \frac{\Gamma_e^W}{M_{W^\pm}}. \quad (3)$$

The W^\pm width not being known experimentally with sufficient accuracy, the theoretical one-loop expression for the leptonic W width in terms of the well-measured Fermi coupling, G_μ , from μ^\pm decay

$$\Gamma_e^W = \frac{G_\mu M_W^3}{6\sqrt{2}\pi(1 + \Delta y^{SC})} \quad (4)$$

is to be inserted in (3) to yield [6]

$$g_{W^\pm}^2(M_{W^\pm}^2) = \frac{4\sqrt{2}G_\mu M_{W^\pm}^2}{1 + \Delta y^{SC}}. \quad (5)$$

The one-loop correction, Δy^{SC} , where SC stands for the change of scale between μ -decay and W-decay, amounts to [1]

$$\begin{aligned}\Delta y^{SC} &= \Delta y_{ferm}^{SC} + \Delta y_{bos}^{SC} \\ &= (-7.79 + 11.1) \times 10^{-3} = 3.3 \times 10^{-3}.\end{aligned}\tag{6}$$

The numerical value is practically independent of the Higgs-boson mass. As indicated in (6), there is a significant cancellation between bosonic and fermionic corrections operative in Δy^{SC} .

3 The improved Born approximation at LEP2.

Supplementing the Born approximation (1), with the coupling constants from (2) and (5), by a Coulomb correction and by initial-state radiation (ISR) in soft-photon approximation [7, 8], the improved Born approximation for LEP2 energies takes the form [1]

$$\begin{aligned}\left(\frac{d\sigma}{d\Omega}\right)_{IBA} &= \frac{\beta}{64\pi^2 s} \left| \frac{2\sqrt{2}G_\mu M_W^2}{1 + \Delta y^{SC}} \mathcal{M}_I^\kappa \delta_{\kappa^-} + 4\pi\alpha(M_Z^2) \mathcal{M}_Q^\kappa \right|^2 \\ &+ \left(\frac{d\sigma}{d\Omega}\right)_{Coul} (1 - \beta^2)^2 + \left(\frac{d\sigma}{d\Omega}\right)_{ISR}.\end{aligned}\tag{7}$$

A detailed numerical comparison between the full one-loop results and the results from the simple representation (7) was carried out in ref. [8] (without the correction Δy^{SC}) and in ref. [1] (taking into account Δy^{SC}). The results are presented in Table 1.

The Table shows the percentage deviation of the IBA (7) from the full-one-loop results for $\Delta y^{SC} = 0$, denoted by Δ_{IBA} , and upon including $\Delta y^{SC} \neq 0$, denoted by $\Delta_{IBA} + \delta\Delta_{IBA}$. Upon including the correction due to Δy^{SC} from (6), the deviations of the improved Born approximation from the full one-loop results are less than 1 % in the full angular range of the production angle between 10 degrees and 170 degrees.

We note that the effect of Δy^{SC} on the cross section can be easily estimated. The cross section (7) being dominated by the part proportional to \mathcal{M}_I , upon neglecting \mathcal{M}_Q in (7), one obtains

$$\delta\Delta_{IBA} \simeq -2\Delta y^{SC} = -0.66\%.\tag{8}$$

This value approximately coincides with the (production-angle-dependent) results in Table 1.

We finally comment on the significance of the appropriate choice of the high-energy scale in the weak coupling, $g_W^\pm(M_W^2)$, with respect to recent one-loop calculations [9] which incorporate the decay of the W^\pm into 4 fermions in a gauge-invariant formulation. These calculations take into account fermion-loops only. While interesting as a first step towards a full one-loop evaluation of $e^+e^- \rightarrow 4$ fermions, the numerical results of a calculation including fermion loops only can easily be estimated within the present framework of stable W^\pm to enlarge the cross section appreciably. In fact, taking into account fermion loops only, the estimate (8) changes sign and becomes

$$\delta\Delta_{IBA}|_{ferm} \simeq -2\Delta y_{ferm}^{SC}|_{m_t=180GeV} \simeq +1.56\%,\tag{9}$$

angle	unpolarized			left-handed		
	Δ_{IBA}	$\delta\Delta_{IBA}$	$\Delta_{IBA} + \delta\Delta_{IBA}$	Δ_{IBA}	$\delta\Delta_{IBA}$	$\Delta_{IBA} + \delta\Delta_{IBA}$
$\sqrt{s} = 161$ GeV						
total	1.45	-0.72	0.73	1.45	-0.72	0.73
10	1.63	-0.73	0.90	1.63	-0.73	0.90
90	1.44	-0.72	0.72	1.44	-0.72	0.72
170	1.26	-0.70	0.56	1.26	-0.70	0.56
$\sqrt{s} = 165$ GeV						
total	1.27	-0.71	0.56	1.28	-0.71	0.57
10	1.67	-0.74	0.93	1.67	-0.74	0.93
90	1.17	-0.71	0.46	1.18	-0.71	0.47
170	0.75	-0.67	0.08	0.77	-0.67	0.10
$\sqrt{s} = 175$ GeV						
total	1.26	-0.71	0.55	1.28	-0.71	0.57
10	1.71	-0.75	0.96	1.71	-0.75	0.96
90	1.03	-0.69	0.34	1.06	-0.70	0.36
170	0.59	-0.62	-0.03	0.69	-0.63	0.06
$\sqrt{s} = 184$ GeV						
total	1.02	-0.70	0.32	1.06	-0.71	0.35
10	1.57	-0.75	0.82	1.57	-0.75	0.82
90	0.67	-0.68	-0.01	0.72	-0.69	0.03
170	0.10	-0.58	-0.48	0.32	-0.64	-0.32
$\sqrt{s} = 190$ GeV						
total	1.24	-0.70	0.54	1.28	-0.71	0.57
10	1.67	-0.74	0.93	1.67	-0.75	0.92
90	0.95	-0.68	0.27	1.01	-0.69	0.32
170	0.58	-0.57	0.01	0.83	-0.59	0.24
$\sqrt{s} = 205$ GeV						
total	1.60	-0.70	0.90	1.65	-0.71	0.94
10	1.77	-0.74	1.03	1.77	-0.74	1.03
90	1.55	-0.66	0.89	1.64	-0.68	0.96
170	1.61	-0.53	1.08	1.94	-0.56	1.38

Table 1: The Table shows the quality of the improved Born approximation (IBA) for the total (defined by integrating over $10^0 \lesssim \vartheta \lesssim 170^0$) and the differential cross section (for W^- -production angles ϑ of 10^0 , 90^0 and 170^0) for $e^+e^- \rightarrow W^+W^-$ at various energies for unpolarized and left-handed electrons. The final percentage deviation, $\Delta_{IBA} + \delta\Delta_{IBA}$, of the IBA from the full one-loop result is obtained by adding the correction $\delta\Delta_{IBA}$ resulting from using the appropriate high energy scale in the SU(2) coupling, to the percentage deviation, Δ_{IBA} , based on using the low-energy scale in the SU(2) coupling, i.e. $\Delta y^{SC} = 0$. (From [1])

and the total deviation from the full one-loop results (using $\Delta_{IBA} \simeq 1.2\%$ from Table 1) rises to values of

$$\Delta_{IBA} + \delta\Delta_{IBA}|_{ferm} \simeq 2.8\%. \quad (10)$$

Accordingly, results from fermion-loop calculations including the decay of the W^\pm are expected to overestimate the cross section by almost 3 % relative to the (so far unknown) outcome of a complete calculation of $e^+e^- \rightarrow 4$ fermions including bosonic loops as well. It is gratifying, that a simple procedure immediately suggests itself for improving the large discrepancy (10). One simply has to approximate the bosonic loop corrections by using the substitution

$$G_\mu \rightarrow G_\mu / (1 + \Delta y_{bos}^{SC}) \quad (11)$$

with $\Delta y_{bos}^{SC} = 11.1 \times 10^{-3}$ in the four-fermion production amplitudes. Substitution (11) practically amounts to using $g_{W^\pm}(M_W^2)$ in four-fermion production as well. With substitution (11), it is indeed to be expected that the deviation of four-fermion production in the fermion-loop scheme will be diminished from the above estimated value of $\simeq 2.8\%$ to a value below 1 %.

4 The high-energy-Born-form approximation (HEBFA) for $e^+e^- \rightarrow W^+W^-$ at one loop.

I turn to W-pair production in the high-energy region to be explored by a future e^+e^- linear collider or by a $\mu^+\mu^-$ collider. The subsequent HEBFA will turn out to be valid at center-of-mass energies above a lower limit of approximately 400 GeV.

Including one-loop corrections [10, 11], the helicity amplitudes for e^+e^- annihilation into W-pairs may be represented in terms of twelve invariant amplitudes

$$\begin{aligned} \mathcal{H}(\sigma, \lambda, \bar{\lambda}) &= S_I^{(\sigma)}(s, t)\mathcal{M}_I(\sigma, \lambda, \bar{\lambda}) + S_Q^{(\sigma)}(s, t)\mathcal{M}_Q(\sigma, \lambda, \bar{\lambda}) \\ &+ \sum_{i=2,3,4,6} Y_i^{(\sigma)}(s, t)\mathcal{M}_i(\sigma, \lambda, \bar{\lambda}). \end{aligned} \quad (12)$$

The structure of the electroweak theory, its renormalizability in particular, restricts (renormalized) ultraviolet and infrared divergences to only affect the invariant amplitudes, $S_I^{(\sigma)}$ and $S_Q^{(\sigma)}$, multiplying the basic matrix elements that are also present in the Born approximation. Accordingly, it is suggestive to approximate [7, 12] the helicity amplitudes (12) in the high-energy limit by dropping all contributions in (12) beyond the ones with a structure identical to the Born approximation. As the bosonic matrix elements do not form an orthonormal vector space, this requirement does not uniquely determine $S_I^{(\sigma)}(s, t)$ and $S_Q^{(\sigma)}(s, t)$. Motivated by the necessary condition of unitarity constraints at high energies, a certain choice of the basic matrix elements was suggested and numerically explored in the early nineties in refs. [7, 12]. More recently it was shown [2] that a somewhat different choice of the basic matrix elements has the advantage of reproducing the amplitudes for production of longitudinal W bosons exactly in the HEBFA. As the production of longitudinal W bosons is dominant at high energies, this novel choice is to be the preferred one.

Moreover, while the previous analysis [7, 12] of the validity of the HEBFA was carried out purely numerically, in the more recent paper [2] simple analytical formulae for the invariant amplitudes $S_I^{(-)}$ and $S_Q^{(\pm)}$ in (12) were presented. Upon including soft-photon radiation, the invariant amplitudes $S_I^{(-)}$ and $S_Q^{(\pm)}$ turn into [2]

$$\hat{S}_{(I,Q)} = S_{(I,Q)}|_{\Delta\alpha, m_t} + S_{(I,Q)}(\Delta E)|_{brens} + S_{(I,Q)}^{dom}. \quad (13)$$

The first term in (13) contains the running of the electromagnetic coupling and the SU(2) breaking due to the top quark. The second term is due to the soft-photon bremsstrahlung, while the third one contains the remaining non-universal loop corrections, in particular all the bosonic loops, in high-energy approximation.

The analytic expressions for $S_{(I,Q)}^{dom}$ were extracted from ref. [13], where cross sections for W-pair production for various helicities were deduced in a systematic high-energy expansion, without the attempt of constructing a Born-form approximation. Replacing subdominant terms (that fill several pages of formulae in ref. [13]) by constants, the expressions deduced for $S_{I,Q}^{dom}$ fit on less than two pages and are presented below:

$$\begin{aligned} S_I^{(-)dom} &= \frac{\alpha}{4\pi s_W^2} \left[-\frac{1+2c_W^2+8c_W^4}{4c_W^2} \left(\log \frac{s}{M_W^2}\right)^2 + \left(4+2\frac{s}{u}\right) \left(\log \frac{s}{M_W^2}\right) \left(\log \frac{s}{t}\right) \right. \\ &- \left(\frac{s[s(1-6c_W^2)+3t]}{4c_W^2(t^2+u^2)} + \frac{s(1-6c_W^2)}{2c_W^2 u} \right) \left(\log \frac{s}{t}\right)^2 \\ &- \frac{3st}{2(t^2+u^2)} \left(\log \frac{s}{u}\right)^2 - \frac{2s}{u} \left(\log \frac{s}{t}\right) \left(\log \frac{s}{u}\right) \\ &+ \frac{3(s_W^4+3c_W^4)}{4c_W^2} \log \frac{s}{M_W^2} - \frac{1-4c_W^2+8c_W^4}{2c_W^2} \left(\log \frac{s}{M_W^2}\right) \left(\log c_W^2\right) \\ &+ 2(1-2c_W^2) \left(\log \frac{t}{u}\right) \left(\log \frac{s}{M_Z^2}\right) - 2s_W^2 \left(\log \frac{t}{u}\right)^2 - 8s_W^2 Sp\left(-\frac{u}{t}\right) \\ &\left. - \frac{s[3s+t+6c_W^2(s+3t)]}{4c_W^2(t^2+u^2)} \log \frac{s}{t} - \frac{(1-6c_W^2)su}{4c_W^2(t^2+u^2)} \right] - 0.012, \end{aligned} \quad (14)$$

$$\begin{aligned} S_Q^{(-)dom} &= \frac{\alpha}{8\pi s_W^2} \left[-\frac{3-4c_W^2+12c_W^4-16c_W^6}{4c_W^2 s_W^2} \left(\log \frac{s}{M_W^2}\right)^2 \right. \\ &+ \frac{56-97c_W^2+76c_W^4-36c_W^6}{6c_W^2 s_W^2} \log \frac{s}{M_W^2} \\ &- (1-2c_W^2) \frac{2(1-2c_W^2)^2+1}{2c_W^2 s_W^2} \log c_W^2 \log \frac{s}{M_W^2} + \left(4+2\frac{1-2c_W^2}{s_W^2} \frac{s}{u}\right) \log \frac{s}{M_W^2} \log \frac{s}{t} \\ &+ \frac{(1-2c_W^2)^3}{c_W^2 s_W^2} \left(\log \frac{u}{t}\right) \left(\log \frac{s}{M_Z^2}\right) - 2\frac{1-2c_W^2}{s_W^2} \frac{s}{u} \left(\log \frac{s}{t}\right) \left(\log \frac{s}{u}\right) \\ &- \left[\frac{1-16c_W^2+20c_W^4}{4c_W^2 s_W^2} \frac{s}{u} + \frac{1-2c_W^2}{4c_W^2 s_W^2} s \frac{s+3t-6c_W^2 s}{t^2+u^2} \right] \left(\log \frac{s}{t}\right)^2 \\ &- \left(\frac{1}{4c_W^2 s_W^2} \frac{s}{t} + \frac{1-2c_W^2}{2s_W^2} \frac{3st}{t^2+u^2} \right) \left(\log \frac{s}{u}\right)^2 \\ &- 4s_W^2 \left(\log \frac{u}{t}\right)^2 - 16s_W^2 Sp\left(-\frac{u}{t}\right) - \frac{1-2c_W^2}{4c_W^2 s_W^2} s \frac{3s+t+6c_W^2(s+3t)}{t^2+u^2} \log \frac{s}{t} \\ &\left. - \frac{(1-2c_W^2)(1-6c_W^2)}{4c_W^2 s_W^2} \frac{su}{t^2+u^2} + \frac{3}{2} \frac{m_t^2}{s_W^2 M_W^2} \log \frac{m_t^2}{s} \right] + 0.030, \end{aligned} \quad (15)$$

$$\begin{aligned}
S_Q^{(+dom)} &= \frac{\alpha}{4\pi} \left[-\frac{5s_W^4 + 3c_W^4}{4c_W^2 s_W^2} \left(\log \frac{s}{M_W^2}\right)^2 + \frac{65s_W^2 + 18c_W^4}{6c_W^2 s_W^2} \log \frac{s}{M_W^2} \right. \\
&- \frac{(1 - 2s_W^2)^2 + 4s_W^4}{2c_W^2 s_W^2} \log c_W^2 \log \frac{s}{M_W^2} \\
&+ 2\frac{1 - 2c_W^2}{c_W^2} \log \frac{u}{t} \log \frac{s}{M_Z^2} + \frac{s}{2c_W^2 u} \left(\log \frac{s}{t}\right)^2 \\
&\left. - \frac{s}{2c_W^2 t} \left(\log \frac{s}{u}\right)^2 - 2\left(\log \frac{u}{t}\right)^2 - 8Sp\left(-\frac{u}{t}\right) + \frac{3m_t^2}{2s_W^2 M_W^2} \log \frac{m_t^2}{s} \right] + 0.045.
\end{aligned} \tag{16}$$

In figs. 1 to 3, [2], for $\sqrt{s} = 500$ GeV and 2000 GeV, I show the invariant amplitudes $\hat{S}_I^{(-)}$ and $\hat{S}_Q^{(\pm)}$ entering the HEBFA. The soft-photon cut-off is chosen as $\Delta E = 0.025\sqrt{s}$. We note that over much of the angular range of the production angle the HEBFA yields a very good approximation of the full one-loop results. The quality of the approximation (obviously) improves with increasing energy. In figs. 1 to 3, we also indicate the results obtained for $\hat{S}_I^{(-)}$ and $S_Q^{(\pm)}$ if only fermion loops and soft-photon radiation is taken into account. The remarkably large difference between the results with only fermion loops and the full corrections is an important genuine effect of electroweak loop corrections. Its large magnitude is due to the squared (non-Abelian Sudakov) logs appearing in the expressions (14) to (16).

We turn to the accuracy of the total cross section, when evaluated in HEBFA. In Table 2, we present the accuracy $\Delta(\%)$ defined by

$$\Delta(\%) = \frac{d\sigma_{appr.} - d\sigma_{full\ one-loop}}{d\sigma_{Born}}. \tag{17}$$

Table 2 first of all shows the accuracy of the Born-form approximation, i.e. dropping all terms beyond the Born form in (12), but evaluating \hat{S}_I and $\hat{S}_Q^{(\pm)}$ at one loop exactly. Secondly, Table 2 shows the result of using the HEBFA for $\hat{S}_I^{(-)}$ and $\hat{S}_Q^{(\pm)}$. We conclude that the accuracy of the HEBFA is excellent, except for the case of mixed polarizations of the W bosons, which is strongly suppressed in magnitude, however. For a detailed discussion of the results for angular distributions, we refer to ref. [2].

5 HEBFA for $e^+e^- \rightarrow W^+W^- \rightarrow 4\text{fermions}(+\gamma)$ at one loop.

In a very recent paper [3], the HEBFA was supplemented by including the decay of the W bosons and hard-photon radiation. Specifically, we looked at the decay channel

$$e^+e^- \rightarrow W^+(u\bar{d})W^-(\bar{s}c)(+\gamma), \tag{18}$$

as well as the semileptonic channel

$$e^+e^- \rightarrow W^+(u\bar{d})W^-(e\bar{\nu})(+\gamma). \tag{19}$$

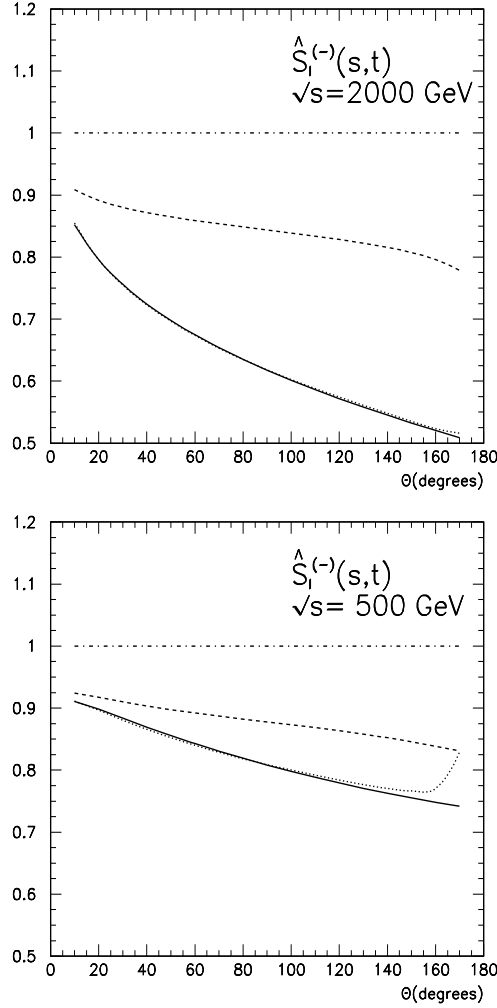


Figure 1: The Born-form invariant amplitude $\hat{S}_l^{(-)}(s, t)$ as a function of the W-production angle, θ , for $\sqrt{s} = 2000\text{GeV}$ and $\sqrt{s} = 500\text{GeV}$ in (i) the full one-loop evaluation including soft-photon bremsstrahlung (solid line), (ii) the fermion-loop approximation including soft-photon bremsstrahlung (dashed line), (iii) the high-energy approximation based on (14) to (16) (dotted line), (iv) the Born approximation (dash-dotted line).

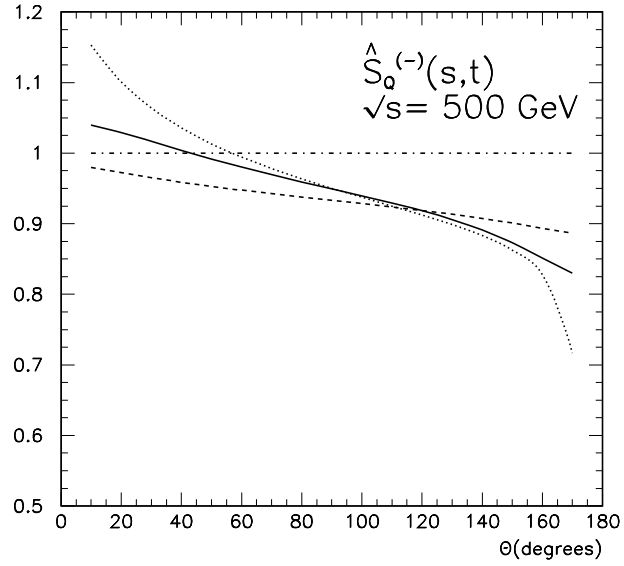
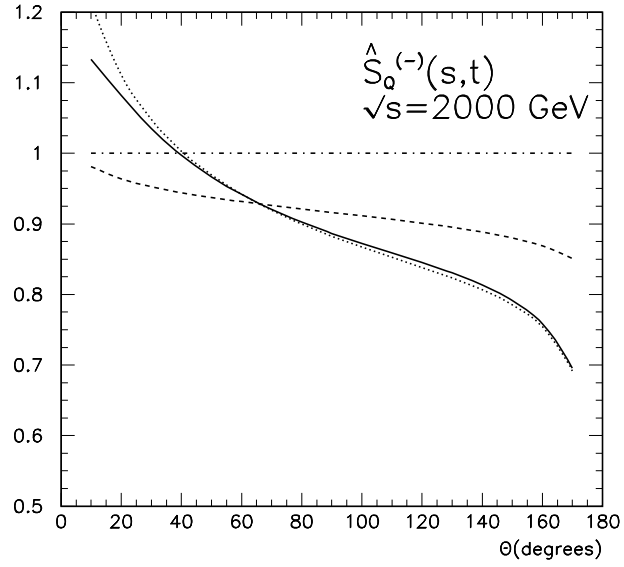


Figure 2: Same as Fig. 1, but for $\hat{S}_Q^{(-)}(s,t)$

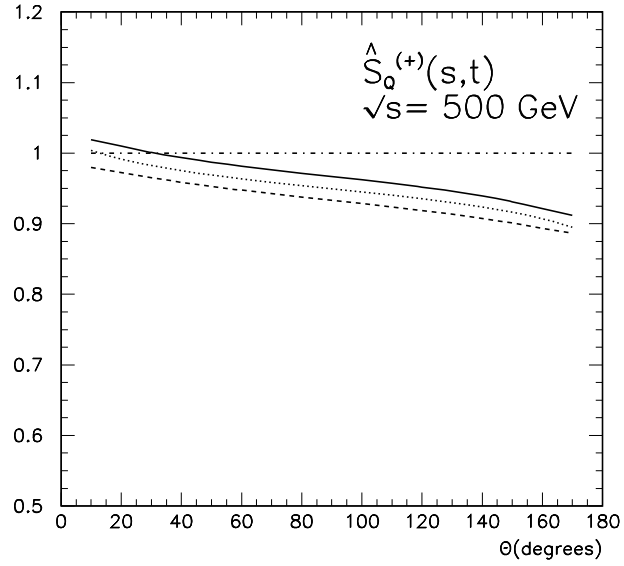
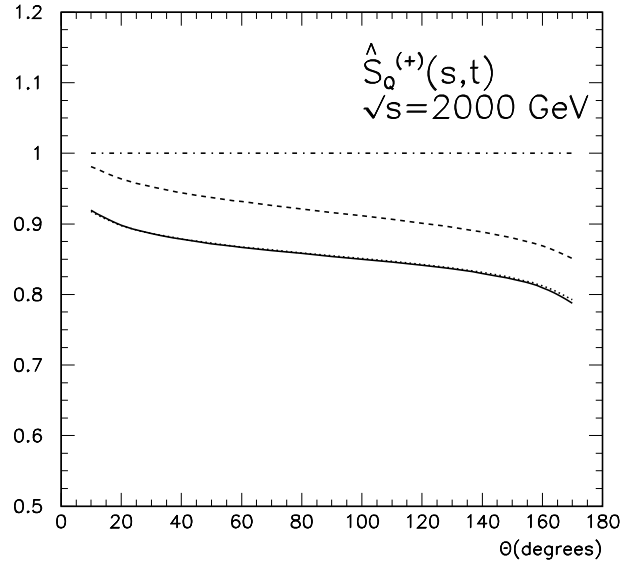


Figure 3: Same as Fig. 1, but for $\hat{S}_Q^{(+)}(s,t)$

angle	High-energy-Born-form approximation		Born-form approximation		full one-loop	Born
	$\sigma(pb)$	$\Delta(\%)$	$\sigma(pb)$	$\Delta(\%)$	$\sigma(pb)$	$\sigma(pb)$
$\sqrt{s} = 2000 \text{ GeV}$						
“unpol.”	1.461×10^{-1}	+0.14	1.461×10^{-1}	+0.16	1.457×10^{-1}	2.758×10^{-1}
transv.	1.422×10^{-1}	+0.19	1.423×10^{-1}	+0.19	1.417×10^{-1}	2.683×10^{-1}
longit.	3.526×10^{-3}	-0.10	3.533×10^{-3}	0.00	3.533×10^{-3}	6.788×10^{-3}
mixed	2.912×10^{-4}	-14.79	2.909×10^{-4}	-14.83	3.833×10^{-4}	6.229×10^{-4}
$\sqrt{s} = 500 \text{ GeV}$						
“unpol.”	3.448	-0.42	3.462	-0.11	3.467	4.545
transv.	3.260	-0.34	3.274	-0.01	3.274	4.294
longit.	8.287×10^{-2}	-0.33	8.323×10^{-2}	0.00	8.323×10^{-2}	1.091×10^{-1}
mixed	1.033×10^{-1}	-3.19	1.034×10^{-1}	-3.13	1.078×10^{-1}	1.419×10^{-1}

Table 2: The total cross section for W^+W^- pair production (obtained by integration over the angular range of the production angle of $10^\circ \leq \vartheta \leq 170^\circ$) at $\sqrt{s} = 2000 \text{ GeV}$ and $\sqrt{s} = 500 \text{ GeV}$. The different rows show the results when summing over the W^+W^- spins (“unpol.”) and the results for the various cases of polarization of the produced W^+ and W^- . The first column shows the result of the HEBFA based on (13) to (16). The second column gives the result of the Born-form approximation obtained by evaluating $\hat{S}_I^{(-)}$ and $\hat{S}_Q^{(\pm)}$ at one-loop level exactly. The third column shows the full one-loop result and the Born approximation.

A two-step procedure was employed in ref. [3]. In a first step, we showed that the background of four-fermion production not proceeding via two W bosons can be suppressed by an appropriate cut,

$$\left| \sqrt{k_\pm^2} - M_W \right| \leq 5\Gamma_W, \quad (20)$$

on the invariant mass $\sqrt{k_\pm^2}$ of the produced fermion pairs. In a tree-level calculation, using GRACE [14], we compared the production of four fermions via intermediate W bosons with the production process

$$e^+e^- \rightarrow u\bar{d}\bar{c}s \quad (21)$$

based on the full set of all contributing diagrams. While in general the introduction of Breit-Wigner denominators in the process (21) leads to problems of gauge invariance (e.g. [8]), the “fixed-width scheme” employed for the background estimate finds some justification in a “complex-mass scheme” [15] and should be sufficiently reliable. The results in Table 3, [3], in particular a comparison of lines 5 and 8, show that the cut (20) on the invariant masses of the fermion pairs removes the non-doubly-resonant background to the level of less than 0.3 %. The suppression of the background in the semileptonic channel is only slightly larger. The results on Δ , corresponding to the last line in table 3, are given by 0.9 %, 0.4 % and 0.4 %, respectively.

We turn to the second step, the calculation of the cross sections for reactions (18), (19) at one loop at collider energies. Extensive calculations have demonstrated [16, 17] that non-factorizable corrections to four-fermion production are small at high energies, as one might expect, and moreover, they vanish upon integration over the invariant masses of the fermion pairs. Accordingly, it is justified to employ one-loop W-pair-production and

Line	\sqrt{s}	500 GeV	1 TeV	2 TeV
1	$\sigma(e^+e^- \rightarrow W^+W^-)$	7.458	2.785	9.421×10^{-1}
Zero width approximation				
2	$\sigma \times BR(W^+ \rightarrow u\bar{d}) \times BR(W^- \rightarrow \bar{c}s)$	8.289×10^{-1}	3.094×10^{-1}	1.047×10^{-1}
Breit-Wigner, full four-fermion phase space				
3	$\sigma(e^+e^- \rightarrow W^+(\rightarrow u\bar{d})W^-(\rightarrow \bar{c}s))$	8.291×10^{-1}	3.097×10^{-1}	1.046×10^{-1}
4	$\sigma(e^+e^- \rightarrow u\bar{d}\bar{c}s)$	8.466×10^{-1}	3.248×10^{-1}	1.124×10^{-1}
5	Difference Δ in %	2.1 %	4.9%	7.5%
Breit-Wigner, restricted phase space, $ \sqrt{k_{\pm}^2} - M_W \lesssim 5\Gamma_W$				
6	$\sigma(e^+e^- \rightarrow W^+(\rightarrow u\bar{d})W^-(\rightarrow \bar{c}s))$	7.264×10^{-1}	2.713×10^{-1}	9.16×10^{-2}
7	$\sigma(e^+e^- \rightarrow u\bar{d}\bar{c}s)$	7.275×10^{-1}	2.717×10^{-1}	9.19×10^{-2}
8	Difference Δ in %	0.1 %	0.1 %	0.3 %

Table 3: Tree-level results in [pb] for W^+W^- -mediated four-fermion production (specifically for the $u\bar{d}\bar{c}s$ final state) compared with four-fermion production including (non-doubly-resonant) background for different phase-space cuts.

-decay amplitudes, when evaluating reactions (18) and (19) at one-loop level. Moreover, non-doubly-resonant contributions are suppressed by imposing the cut (20).

In detail, the numerical results [3] to be presented are based on

- i) one-loop on-shell W^+W^- production and decay amplitudes, based on the full one-loop results from [18] as well as the HEBFA from [2],
- ii) fixed-width Breit-Wigner denominators and the phase-space cut (20), i.e. a double-pole approximation with respect to four-fermion production,
- iii) inclusion of hard-photon emission generated by GRACE [14] and the Monte Carlo routine BASES [19],
- iv) independence of the soft-photon cut-off ΔE for $1\text{GeV} < \Delta E < 10\text{GeV}$.

With canonical values for the input parameters, $M_Z = 91.187\text{GeV}$, $M_W = 80.22\text{GeV}$, $M_H = 200\text{GeV}$, the results in Tables 4 to 6 were obtained.

Table 4 demonstrates that indeed at $\sqrt{s} = 1\text{TeV}$, the deviation

$$\Delta = \frac{\frac{d\sigma}{d\cos\vartheta}(\text{HEBFA}) - \frac{d\sigma}{d\cos\vartheta}(\text{exact})}{\frac{d\sigma}{d\cos\vartheta}(\text{exact})} < 0.5\% \quad (22)$$

is less than 0.5 %, except for very forward and very backward production angles ϑ . Finally, Table 5 and Table 6 show the energy dependence of the total cross section. Upon applying the angular cut, $10^0 < \vartheta < 170^0$, the accuracy of the total cross section becomes better than 0.3 % for c.m.s. energies above 500 GeV.

Finally, comparing the results of taking into account only fermion loops and photon radiation with the results from the full one-loop calculation, one finds [3] differences that reach approximately 20 % at 2 TeV c.m.s. energy. Accuracies of future experiments of this order of magnitude will accordingly be able to “see” the non-Abelian loop corrections displayed in (14) to (16).

$\cos \theta$	$e^+e^- \rightarrow W^+W^-$	$e^+e^- \rightarrow W^+(ud)W^-(\bar{c}s)$	$e^+e^- \rightarrow W^+(ud)W^-(\bar{c}s) + \gamma$		
	Born	Born	one-loop		
			HEBFA	exact	$\Delta(\%)$
0.95	5.981×10^0	5.827×10^{-1}	2.900×10^{-1}	2.878×10^{-1}	0.76
0.9	2.785×10^0	2.713×10^{-1}	1.211×10^{-1}	1.208×10^{-1}	0.24
0.8	1.207×10^0	1.176×10^{-1}	4.557×10^{-2}	4.557×10^{-2}	0.00
0.7	7.003×10^{-1}	6.826×10^{-2}	2.383×10^{-2}	2.385×10^{-2}	-0.05
0.6	4.597×10^{-1}	4.483×10^{-2}	1.437×10^{-2}	1.438×10^{-2}	-0.02
0.5	3.246×10^{-1}	3.165×10^{-2}	9.429×10^{-3}	9.435×10^{-3}	-0.06
0.4	2.414×10^{-1}	2.352×10^{-2}	6.570×10^{-3}	6.576×10^{-3}	-0.10
0.3	1.869×10^{-1}	1.821×10^{-2}	4.798×10^{-3}	4.808×10^{-3}	-0.20
0.2	1.497×10^{-1}	1.458×10^{-2}	3.645×10^{-3}	3.651×10^{-3}	-0.17
0.1	1.234×10^{-1}	1.201×10^{-2}	2.855×10^{-3}	2.861×10^{-3}	-0.22
0.0	1.041×10^{-1}	1.013×10^{-2}	2.292×10^{-3}	2.297×10^{-3}	-0.23
-0.1	8.941×10^{-2}	8.695×10^{-3}	1.872×10^{-3}	1.876×10^{-3}	-0.22
-0.2	7.766×10^{-2}	7.551×10^{-3}	1.542×10^{-3}	1.544×10^{-3}	-0.16
-0.3	6.773×10^{-2}	6.586×10^{-3}	1.268×10^{-3}	1.269×10^{-3}	-0.05
-0.4	5.883×10^{-2}	5.721×10^{-3}	1.031×10^{-3}	1.030×10^{-3}	0.06
-0.5	5.036×10^{-2}	4.897×10^{-3}	8.174×10^{-4}	8.148×10^{-4}	0.31
-0.6	4.188×10^{-2}	4.073×10^{-3}	6.202×10^{-4}	6.155×10^{-4}	0.77
-0.7	3.305×10^{-2}	3.214×10^{-3}	4.364×10^{-4}	4.291×10^{-4}	1.70
-0.8	2.360×10^{-2}	2.295×10^{-3}	2.680×10^{-4}	2.573×10^{-4}	4.14
-0.9	1.333×10^{-2}	1.296×10^{-3}	1.215×10^{-4}	1.074×10^{-4}	13.19

Table 4: The angular distribution of W-pair production at the energy $\sqrt{s} = 2E_{beam} = 1$ TeV in units of pb . The first column shows the Born cross section for $e^+e^- \rightarrow W^+W^-$. The second column shows the results of treating W production and decay in Born approximation and integrating the Breit-Wigner distribution over the restricted interval (20). The third and the fourth column are obtained by using the one-loop amplitudes for production and decay, again, integrating the Breit-Wigner distribution over the restricted interval (20). A soft-photon cut $\Delta E/E = 0.01$ is used for the one-loop results. The HEBFA is used for the third column and the full one-loop amplitudes are used for the fourth column. The last column gives the results for the relative deviation, Δ , from (22).

E_{beam}	$e^+e^- \rightarrow W^+W^-$	$e^+e^- \rightarrow W^+(ud)W^-(\bar{c}s)$	$e^+e^- \rightarrow W^+(ud)W^-(\bar{c}s) + \gamma$		
	Born	Born	one-loop		
			HEBFA	exact	$\Delta(\%)$
200	8.698	0.8467	0.8718	0.8794	-0.9
300	5.091	0.4958	0.5275	0.5262	0.2
400	3.384	0.3295	0.3575	0.3533	1.2
500	2.433	0.2370	0.2602	0.2556	1.8
600	1.844	0.1795	0.1996	0.1951	2.3
700	1.452	0.1413	0.1584	0.1543	2.7
800	1.177	0.1145	0.1292	0.1259	2.6
900	0.9750	0.09485	0.1080	0.1044	3.4
1000	0.8228	0.08010	0.0915	0.0881	3.9

Table 5: The energy dependence of the $(ud\bar{d})(\bar{c}s)$ - production cross section in DPA. The second column is the Born cross section, while the third column gives the one-loop cross section including hard-photon radiation. The deviation, Δ , defined in analogy to (22), quantifies the discrepancy between the HEBFA and the full one-loop results.

E_{beam}	$e^+e^- \rightarrow W^+W^-$	$e^+e^- \rightarrow W^+(ud)W^-(\bar{c}s)$	$e^+e^- \rightarrow W^+(ud)W^-(\bar{c}s) + \gamma$		
	Born	Born	one-loop		
			HEBFFA	exact	$\Delta(\%)$
200	6.724	0.6561	0.6746	0.6794	-0.71
300	3.042	0.2964	0.3109	0.3109	0.00
400	1.695	0.1654	0.1725	0.1721	0.23
500	1.077	0.1051	0.1085	0.1082	0.28
600	0.7440	0.07262	0.07405	0.07383	0.30
700	0.5449	0.05318	0.05349	0.05334	0.28
800	0.4162	0.04063	0.04027	0.04015	0.30
900	0.3284	0.03205	0.03136	0.03127	0.29
1000	0.2657	0.02593	0.02505	0.02498	0.28

Table 6: As Table 5, but with a restriction on the W^+W^- production angle that is given by $10^\circ < \theta < 170^\circ$.

6 Conclusions

The main points of this review may be summarized as follows:

- i) Concerning the LEP2 energy range, the simple procedure of introducing the SU(2) gauge coupling $g_{W^\pm}(M_W^2)$ at the high-energy scale, approximated by the W-mass-shell condition $s \simeq M_W^2$, and the electromagnetic coupling $\alpha(M_Z^2)$, allows one to incorporate most of the electroweak virtual radiative corrections to $e^+e^- \rightarrow W^+W^-$ in a simple Born formula.
- ii) The detailed numerical results obtained at tree-level at high energies show that a cut of about five times the W width on fermion-pair masses enhances production via W-pairs, reducing non-resonant background to below 0.2 % for $e^+e^- \rightarrow W^+(u\bar{d})W^-(\bar{c}s)$ and below 0.4 % for $e^+e^- \rightarrow W^+(u\bar{d})W^-(e^-\bar{\nu})$. It is accordingly sufficient to concentrate on $e^+e^- \rightarrow W^+W^- \rightarrow 4\text{fermions}$ (i.e. the double-pole approximation) and ignore background contributions, even more so, as in four-fermion production the main interest lies in the test of the non-Abelian gauge-boson interactions of the electroweak theory.
- iii) The HEBFA is excellent for $\sqrt{s} \gtrsim 400\text{GeV}$, provided very-forward and very-backward production is excluded. It is conceptually simple, its analytic expressions fit on two pages, and it is practically important due to a significant reduction in computer time in comparison with the full one-loop calculation.
- iv) Accuracies of future experiments of the order of magnitude of 10 % in the total cross section at TeV energies allow one to isolate bosonic loop corrections.

References

- [1] M. Kuroda, I. Kuss and D. Schildknecht, Phys. Lett. B409 (1997) 405; D. Schildknecht, in Proc. of the Joint Particle Physics Meeting, Ouranopolis, Greece, Sept. 1997, p. 63, ed. A. Nicolaidis.
- [2] M. Kuroda and D. Schildknecht, Nucl. Phys. B531 (1998) 24.

- [3] M. Kuroda, Y. Kurihara and D. Schildknecht, hep-ph/9908486, to appear in Nucl. Phys. B.
- [4] M. Kuroda and D. Schildknecht, Acta Physica Polonica B, Vol. 30 (1999) 3325.
- [5] A. Denner, S. Dittmaier, M. Roth and D. Wackerroth, hep-ph/9912447.
- [6] S. Dittmaier, D. Schildknecht and G. Weiglein, Nucl. Phys. B465 (1996) 3.
- [7] M. Böhm, A. Denner and S. Dittmaier, Nucl. Phys. B376 (1992) 29; B391 (1993) 483 (E).
- [8] W. Beenakker et al., in Physics at LEP2, eds. G. Altarelli, T. Sjöstrand and F. Zwirner, CERN 96-01 Vol. 1, p. 79, hep-ph/9602351.
- [9] W. Beenakker et al., Nucl. Phys. B500 (1997) 255.
- [10] J. Fleischer, F. Jegerlehner and M. Zrałek, Z. Phys. C42 (1989) 409.
- [11] M. Böhm, A. Denner, T. Sack, W. Beenakker, F.A. Berends and H. Kniif, Nucl. Phys. B304 (1988) 463.
- [12] J. Fleischer, J.L. Kneur, K. Kołodziej, M. Kuroda and D. Schildknecht, Nucl. Phys. B378 (1992) 443; B426 (1994) 246 (E).
- [13] W. Beenakker, A. Denner, S. Dittmaier, R. Mertig and T. Sack, Nucl. Phys. B410 (1993) 245.
- [14] T. Ishikawa et al., GRACE manual vers. 1.0, 1993.
- [15] A. Denner, S. Dittmaier, M. Roth, D. Wackerroth, hep-ph/9904472.
- [16] V.S. Fadin and V.A. Khoze, Sov. J. Nucl. Phys. 48 (1988) 309; V.S. Fadin, V.A. Khoze and A.D. Martin, Phys. Lett. B311 (1993) 311; V.S. Fadin et al., Phys. Rev. D52 (1995) 1377.
- [17] A. Denner, S. Dittmaier, M. Roth, Nucl. Phys. B519 (1998) 39; Phys. Lett. B429 (1998) 145.
- [18] M. Kuroda, Analytic expression of the radiative corrections to the process $e^+e^- \rightarrow W^+W^-$ in one-loop order, 1994, unpublished. On request, the computer program is available from the author.
- [19] S. Kawabata, Comput. Phys. Communi. 41 (1986) 127; *ibid.* 88 (1995) 309.